LiDAR Through Domes: Modelling, Simulation, and Correction of Refraction

Pasindu Ranasinghe
School of Minerals and Energy Resources Engineering
University of New South Wales
Sydney, Australia
pasindu.ranasinghe@unsw.edu.au

Dibyayan Patra
School of Minerals and Energy Resources Engineering
University of New South Wales
Sydney, Australia
d.patra@unsw.edu.au

Bikram Banerjee
School of Surveying and Built Environment
University of Southern Queensland
Toowoomba, Australia
bikram.banerjee@unisq.edu.au

Simit Raval
School of Minerals and Energy Resources Engineering
University of New South Wales
Sydney, Australia
simit@unsw.edu.au

***Abstract*— LiDAR plays a vital role in precision sensing, but maintaining accuracy becomes challenging when the sensor is housed within a protective enclosure. Transparent covers, such as polycarbonate domes, introduce beam deflections due to refraction — a factor that is often overlooked — which leads to spatial distortion in the resulting point cloud. This study presents an analytical and experimental investigation of these distortions using a Livox Avia solid-state LiDAR enclosed in a 6 mm thick polycarbonate hemispherical dome. Beam deflections were modelled using Snell's law in MATLAB, simulated in COMSOL Multiphysics, and validated through controlled indoor experiments conducted at distances ranging from 2 m to 5 m. Both MATLAB and COMSOL results showed consistent angular deviation patterns, reinforcing the reliability of the modelling framework. Even small angular deviations can cause dimensional errors of up to 1.4%, with errors increasing further at longer distances. To address this, an angle-based correction strategy is proposed. The approach uses precomputed correction factors to adjust measured points in post-processing, reducing dimensional errors by up to 42.8% at 5 m. The method is lightweight, computationally efficient, and can be directly integrated into existing LiDAR firmware. This enables precise 3D mapping despite enclosure-induced distortion, supporting the practical use of LiDAR in sealed or shielded configurations.**

Keywords*— *enclosure distortion, LiDAR refraction, beam deflection, refraction correction

I. INTRODUCTION

LiDAR systems are widely used across diverse fields such as autonomous navigation, industrial automation, surveying, environmental monitoring, and mining. In many of these applications, the operating environment is harsh, with exposure to dust, moisture, and mechanical impact [1]. To ensure reliable and continuous operation, LiDAR units are typically enclosed in transparent housings. In hazardous environments, such as underground mines or chemical processing facilities, these enclosures must also be certified to meet explosion-proof and safety standards [2]. A hemispherical dome is one such enclosure, offering uniform coverage and structural strength. However, when a LiDAR beam passes through a curved transparent surface, it undergoes refraction, which can affect the accuracy of spatial measurements.

Despite the widespread use of LiDAR across industries, only a few studies have systematically investigated the impact of enclosures on measurement accuracy. In automotive systems, for example, in-cabin LiDAR sensors have been shown to suffer significant signal loss of up to 90% due to infrared-blocking coatings on windshields [3]. A capstone project at the University of Colorado Boulder suggested that distortions from protective domes were negligible [4]. This assumption may not hold in real-world conditions where sensors operate over longer distances or behind thick enclosures. Under such circumstances, the resulting optical distortions can become non-linear and substantial. Biertümpfel et al. specifically emphasised that curved protective windows introduce measurable angular and spatial errors, particularly in high-precision and long-range LiDAR applications, where such effects can no longer be considered optically neutral [5].

While these findings acknowledge the challenges posed by enclosures, detailed investigations into LiDAR systems operating within enclosed environments remain significantly limited, and none, to our knowledge, has focused specifically on solid-state LiDARs. Importantly, existing studies do not propose correction strategies for the optical distortion introduced by such curved protective covers. This gap motivates the present study, which aims to quantify dome-induced errors and apply a correction method based on refraction principles to recover accurate 3D point clouds.

To address this gap, we present a combined analytical and experimental investigation of solid-state LiDAR performance through a polycarbonate dome. The study models beam deflection using Snell's Law, validates these effects using COMSOL Multiphysics simulations, and evaluates them through controlled laboratory experiments. We also propose a simple yet effective angle-based correction strategy to compensate for distortion. Results show that while angular deviations are significant, especially at longer ranges, the proposed correction method successfully reduces spatial error by up to 42.8% at a distance of 5 metres. This makes the method suitable for real-world systems where compact, enclosed LiDAR integration is needed for environmental protection, mobile platforms, or explosion-proof safety compliance.

This work is supported by the Key Science and Technology Innovation Project of China Coal Technology & Engineering Group Corp under Grant No. 2022-3-KJHZ005 and was conducted in collaboration with Beijing Tianma Intelligent Control Technology Co., Ltd.

II. METHODS

A. Sensor and Enclosure Description

This study uses the Livox Avia as the primary LiDAR sensor. It is a compact, solid-state LiDAR designed for high-precision applications. It operates at 905 nm and provides up to 240,000 points per second in single return mode. The sensor covers a horizontal field of view (FOV) of 70.4° and a vertical FOV of 77.2°, using a non-repetitive scanning pattern. Internally, the Livox Avia features a hybrid scanning mechanism that combines a swing mirror and a spinning polygon mirror. As shown in Fig. 1, the laser pulse from the emitter is first deflected vertically by the swing mirror and then redirected horizontally by the rotating polygon mirror to cover the field of view in a pseudo-random pattern.

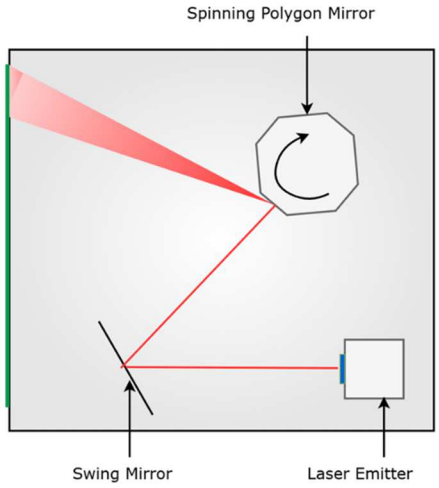

Fig. 1. Internal scanning configuration of the Livox Avia. The laser beam from the emitter is first reflected by a swing mirror (vertical deflection), then redirected by a spinning polygon mirror (horizontal deflection) to scan the environment through a single exit point

Although the scanning pattern changes over time, the laser beams consistently exit through a common optical aperture at the front of the sensor. The internal beam direction varies due to the rotation of the polygon mirror; however, the laser consistently reflects off the same point on the mirror surface (Fig. 1). As a result, the effective origin of the beams remains fixed in space. This makes it reasonable to model LiDAR as a point source for beam direction estimation and optical correction. Adopting this assumption significantly simplifies the analysis, simulation, and correction of refraction effects introduced by the enclosure.

To study the effect of refraction on the LiDAR beams, the sensor was mounted inside a custom-made hemispherical enclosure, made of optical-grade polycarbonate. The dome had an inner diameter of 153 mm and an outer diameter of 165 mm, resulting in a uniform wall thickness of 6 mm. With a refractive index of 1.57 at 905 nm, the material caused the laser beams to bend as they passed through.

The global coordinate system serves as the primary reference frame for all geometrical and physical quantities in this study. It follows a right-handed 3D Cartesian convention, with the origin placed at the centre of the dome's base. In this system, the Z-axis points upward, the X-axis extends forward, and the Y-axis points sideways, forming an orthogonal set of axes (Fig. 2).

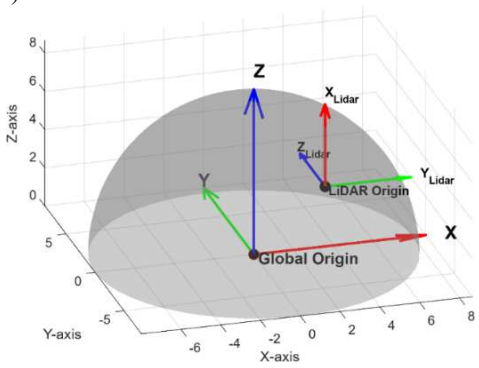

Fig. 2. Global coordinate frame fixed at the center of the dome, and a LiDAR sensor modelled as a point with its local coordinate frame. Both frames follow a right-handed convention with axes colour coded as red (X), green (Y), and blue (Z).

B. Analytical Modelling Using MATLAB

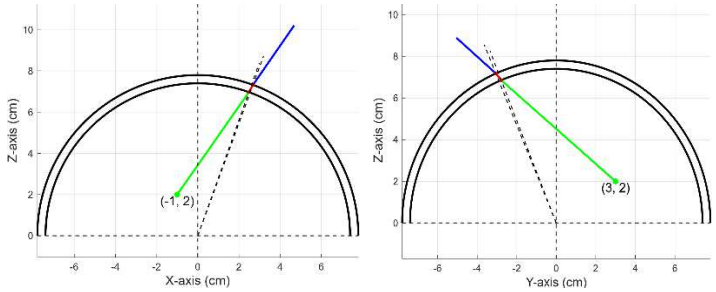

(a) (b)

Fig. 3. 2D projections of the 3D LiDAR beam (−1, 3, 2) + t (−0.40, 0.40, 0.82): (a) XZ-plane view at 55° to X-axis, (b) YZ-plane view at 140° to Y-axis

The LiDAR's conical scanning pattern was decomposed into 2D cross-sectional projections along the XZ and YZ planes, as shown in Fig. 3. This reduction allowed the simulation to focus on planar slices of the beam path, making geometric and optical analysis more tractable while preserving the key behaviour of the system.

The simulation then tracked the path of a laser beam emitted by the LiDAR as it passed through the curved dome. The beam, defined by a known emission position and angle, was intersected with the dome surface. At each point, the surface normal was calculated to determine the local angle of incidence. Snell's Law was applied at both the air-solid and solid-air interfaces to compute the corresponding refraction angles based on the change in refractive index:

$$n_1 \sin(\theta_1) = n_2 \sin(\theta_2) \quad (1)$$

In this equation, n_1 and n_2 are the refractive indices of the first and second media, respectively, such as air and glass. θ_1 is the angle of incidence, and θ_2 is the angle of refraction. Both angles are measured with respect to the normal at the point of intersection.

The ray's direction was updated as it entered and exited the dome, enabling full tracing of the beam through the enclosure

(Fig. 3). From these simulations, the deflection angle—defined as the angular difference between the emitted and exit directions—was calculated. This angle quantifies the optical deviation introduced by the enclosure and directly impacts the accuracy of the LiDAR's spatial measurements. The magnitude of the deflection depends on both the initial emission angle and the position of the LiDAR relative to the dome surface.

C. COMSOL Simulation

A physics-based simulation was performed using COMSOL Multiphysics. The Ray Optics Module was used to simulate laser beams emitted from the LiDAR sensor toward the dome. The spherical shell representing the dome was modelled with accurate physical dimensions, and refraction was automatically computed at each interface using the material's optical properties (Fig. 4). This provided a detailed spatial visualisation and quantitative data to compare with the angular deviations obtained from the MATLAB model. Additionally, the simulation produced estimates of signal attenuation and generated a spot diagram on the XY plane, illustrating the beam spread after passing through the dome.

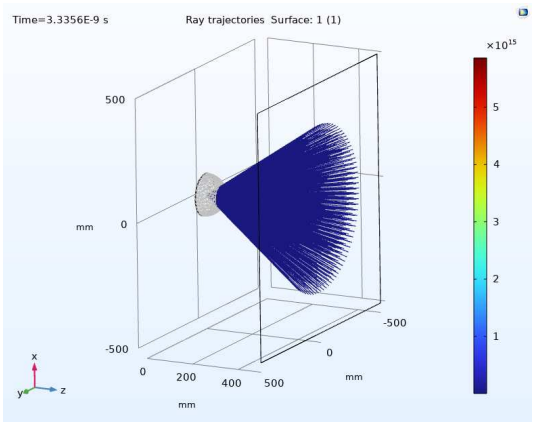

Fig. 4. Ray tracing simulation through the polycarbonate dome using COMSOL Multiphysics. A flat surface is placed in front of the dome to capture the resulting spot diagram.

D. Experimental Setup

The LiDAR and dome enclosure were securely mounted on a tripod, with their relative positioning carefully measured. Experiments were conducted indoors under controlled conditions to minimise external interference. A rectangular target (0.45 m in height and 0.35 m in width) was placed at distances of 2 m, 3 m, 4 m, and 5 m from the sensor. Both the sensor and the target remained fixed during data collection. Point clouds were recorded for 1 second at each distance for both scenarios, with and without the dome. The height and width of the target were extracted from the point cloud data, and the measurements obtained without the dome were treated as ground truth for evaluating enclosure-induced distortion.

E. Correction Strategy

An angle-based correction strategy was developed to compensate for beam deflection caused by refraction. A correction factor table was generated for each fixed position of the LiDAR inside the dome, accounting for deflection in both the XY and YZ planes. These correction factors were derived through MATLAB simulations and validated with COMSOL simulations.

For every point in the captured point cloud, the initial beam direction was calculated from its 3D coordinates and decomposed into XY and YZ plane angles (Fig. 3). These angles were originally defined in the LiDAR's local coordinate frame and were transformed into the global coordinate frame of the dome. Using the transformed angles, the corresponding correction factors were retrieved from the precomputed table. The corrected angles were then used to recalculate the true 3D coordinates of each point, resulting in a refraction-adjusted point cloud.

III. Results

A. Simulation Results

The deflection curves derived from both MATLAB and COMSOL simulations exhibit similar deflection behaviour. While both tools produce comparable patterns in the XZ and YZ planes, COMSOL offers additional parameters, such as beam power distribution, which are discussed in later sections of the results.

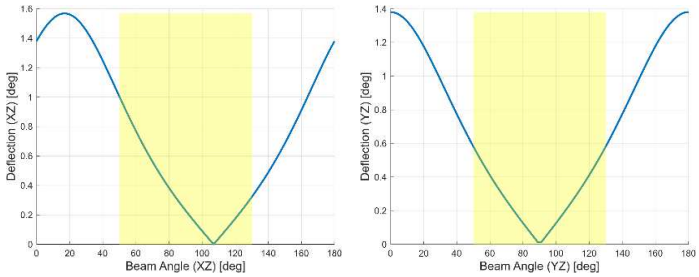

(a) (b)

Fig. 5. (a) Total angular deflection in the XZ plane (b) Total angular deflection in the YZ plane; The yellow region indicates the scanning angle range of the Livox LiDAR.

Fig. 5 illustrates the deflection angles of LiDAR beams when the sensor is fixed at the global coordinate position, P_1 = (–1.615, 0, 5.3) cm, matching the physical mounting location used in the experimental setup. The sensor is symmetrically aligned along the Y = 0 axis and positioned closer to the dome's left inner surface. This configuration results in a symmetric deflection profile in the YZ plane (Fig. 5b), due to equal incident angles on both sides of the dome. The minimum deflection occurs at 90°, where the rays are perpendicular to the dome surface and thus experience minimal bending.

In contrast, the deflection profile in the XZ plane (Fig. 5a) is asymmetric. This is a result of the sensor being offset from the geometric centre along the X-axis, which causes beams on one side to interact with the dome at steeper incident angles than those on the opposite side.

Deflection is defined as the angular difference between the emergent and incident ray directions relative to the local surface normal. Since all beams refract away from the normal as they exit the dome, deflection values are always positive. The degree of deflection varies with the angle of incidence and the beam's relative position within the enclosure.

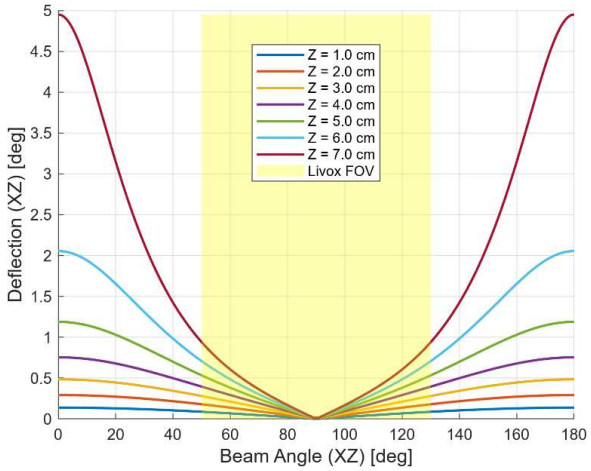

Fig. 6. Deflection curves in the XZ plane as the LiDAR is moved along the Z-axis, from the centre towards the dome surface.

Fig. 6 illustrates how beam deflection varies as the LiDAR sensor is repositioned along the Z-axis. The deflection curves remain symmetric about 90°, since the sensor stays aligned with the dome's central vertical axis, resulting in equal incident angles on both sides. As the Z-offset increases, the rays strike more curved regions of the dome at steeper angles, leading to greater refraction. This results in a consistent, symmetric curve with increasing magnitude. A similar effect is observed in the YZ plane.

However, when the sensor is moved along the X or Y axis, the deflection pattern in the XZ or YZ plane, respectively, shifts laterally and loses symmetry about 90° (Fig. 5a). While the shape of the deflection curve remains consistent, its centre shifts in the direction of the sensor offset due to asymmetrical beam interactions with the dome surface.

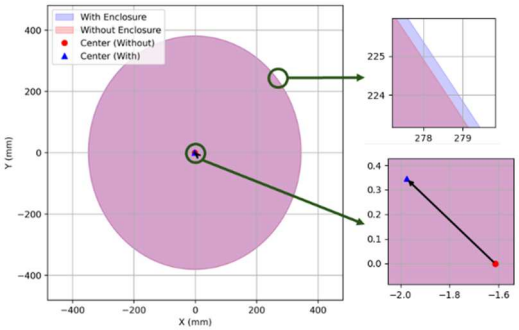

Fig. 7. Beam distribution at 50 cm from the LiDAR: red without enclosure, yellow with enclosure. Zoomed views show increased spread (top) and centre offset due to the enclosure (bottom).

The COMSOL simulation provides additional insights beyond angular deflection. When the sensor is positioned at P_1 the projected beam distribution on a surface placed 50 cm in front of the sensor exhibits a distinct elliptical shape (Fig. 7). The beam expands by approximately 0.45 mm in both height and width due to non-uniform refraction across the dome's curved surface. The centre of the distribution shifts by a total of 0.5 mm diagonally, moving leftward and upward from its original position. Additionally, the simulation shows that ~ 9.6% of the LiDAR beam power is lost as it passes through the enclosure, primarily due to absorption by the polycarbonate material.

B. *Experimental Results*

The height and width of the object were measured directly from the LiDAR point cloud, while the distance to the object was determined using the X-coordinate of the LiDAR points. These values were then compared against ground truth measurements obtained without the enclosure. This comparison, as illustrated in Fig. 8, provides a basis to evaluate how the enclosure affects the accuracy of both dimensional and range estimates. The relative error for each measurement was calculated using the following expression.

$$Relative\ Error\ (\%) = \left(\frac{Measured\ with\ Enclosure - Measured\ without\ Enclosure}{Measured\ without\ Enclosure}\right) x\ 100 \quad (2)$$

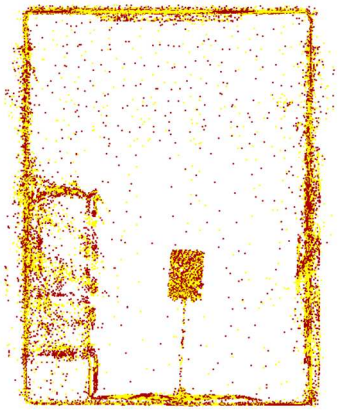

Fig. 8. Point cloud overlay at 2 m: red without enclosure, yellow with enclosure. The rectangular target board is visible at the centre

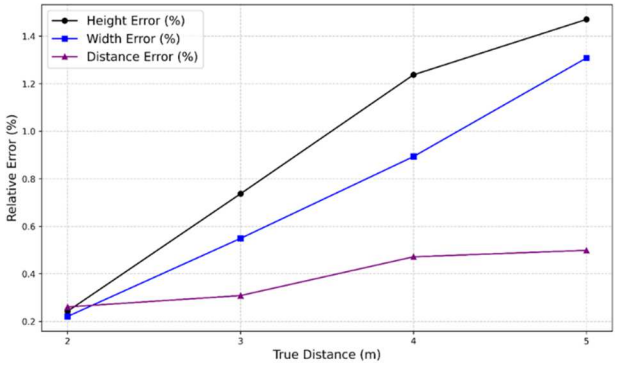

Fig. 9: Relative errors in object height, width, and distance—estimated from point clouds with the enclosure—compared across varying LiDAR-to-object distances.

Based on the results (Fig. 9), all the relative errors are positive, indicating that the dome enclosure tends to slightly increase the measured values in all dimensions. The height error increases most significantly with distance, which can be attributed to the vertical beam divergence of the Livox Avia (0.28°). As the laser beams travel further, they spread more in the vertical direction. The width error also increases with distance, but at a more moderate rate. This aligns with the sensor's much smaller horizontal beam divergence of 0.03°, resulting in a narrower spread and reduced sensitivity to enclosure-induced distortion in the horizontal plane. However, the results also suggest that while higher beam divergence

contributes to greater measurement error, the relationship is not strictly proportional.

The distance error, on the other hand, remains small and stable across all measured distances. Since LiDAR determines range using time-of-flight, the dome does not significantly alter this measurement, aside from introducing a small, constant bias due to the change in optical path length as the beam passes through the dome material. This bias is consistent across all distances, which explains the nearly flat trend in relative distance error seen in the plot.

The next set of results presents the average relative error in the measured height and width of the object. The reported error reflects the mean of these two dimensions at each evaluated distance. As shown in Fig. 10, the results exhibit reasonable agreement between simulation and experimental data, with percentage differences remaining within ±25%, thereby supporting the validity of the simulation. The experimental measurements were consistently higher than the simulated values.

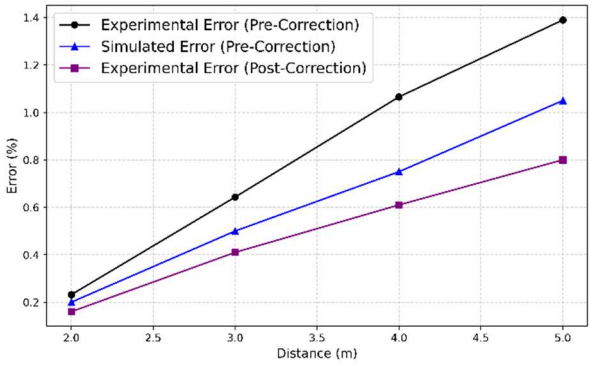

Fig. 10: Comparison of relative errors in simulated and experimental measurements before and after correction.

Although the deflection angles were small, their spatial impact increased with distance, resulting in larger positional deviations on the target surface. Consequently, the relative error in object dimensions rose progressively from 0.3% to 1.4% as the distance increased to 5 m. The proposed correction method significantly improved accuracy, reducing the error from 1.4% to 0.8% at 5 m, an overall reduction of 42.8%.

IV. Discussion

This study presents the first systematic analysis and correction of LiDAR beam deflection through a transparent dome enclosure, specifically focusing on solid-state LiDAR systems. The results demonstrate that even minor angular deviations caused by refraction can lead to measurable spatial distortions in point cloud data. These effects become increasingly pronounced with distance, where small beam deflections translate into larger positional errors on target surfaces. As demonstrated in the experimental results, the enclosure introduces consistent overestimations in measured object dimensions, with height measurements showing greater sensitivity due to the sensor's larger vertical beam divergence.

The proposed angle-based correction strategy proved effective in mitigating the dimensional errors caused by refraction. It reduced the average relative error by 42.8%, demonstrating strong potential for improving measurement accuracy. This level of improvement is particularly significant for applications that rely on precise dimension estimation, such as object detection, robotic navigation, and 3D mapping in enclosed or explosion-proof environments.

Importantly, this research establishes a practical and lightweight method that can be implemented directly within the LiDAR's firmware or applied as a post-processing step in point cloud pipelines. The correction approach does not rely on external calibration targets or complex machine learning models, making it attractive for field deployment in rugged environments such as underground mines, industrial facilities, or mobile robotic platforms.

However, the study also presents certain limitations. The current model focuses solely on refraction effects and assumes ideal conditions such as uniform material properties and a perfectly hemispherical dome. In real-world scenarios, additional factors such as surface imperfections, dust accumulation, temperature-dependent index variations, and multi-path reflections can further degrade accuracy. These factors were not accounted for in the present analysis.

Another simplification involves treating the LiDAR as a single-point source. In reality, the beam originates from a small region within the sensor housing, and the exact optical origin may shift depending on the internal scanning mechanism. This could introduce minor discrepancies in angle estimation, especially at steep beam angles or close to the enclosure surface.

Additionally, while COMSOL simulations indicated that approximately 9.6% of the LiDAR power is lost during transmission through the dome, this was not quantitatively verified in the experiments. Power loss and its impact on point cloud density and intensity remain areas for further investigation.

Future work could extend this framework by incorporating more advanced optical models that consider beam divergence, reflection, and absorption. The methodology could also be adapted to non-spherical enclosures or integrated with learning-based correction for complex or dynamic conditions.

V. Conclusion

This study addressed the often-overlooked issue of optical distortion introduced by curved protective enclosures in LiDAR systems, with a specific focus on solid-state LiDAR. We demonstrated that such distortions, while frequently considered negligible, can significantly impact measurement accuracy in real-world scenarios involving long-range sensing and complex refractive surfaces. By applying a correction method based on refraction principles, we were able to recover more accurate 3D point cloud data. These findings highlight the importance of

accounting for enclosure effects in both hardware design and data processing pipelines and lay the groundwork for future efforts in refining correction models and validating them across diverse sensor types and enclosure geometries.

ACKNOWLEDGMENT

We thank Amantha Mawathwage (Temporary Lecturer, Department of Mechanical Engineering, University of Moratuwa) for his support in COMSOL simulations. We also acknowledge Kanchana Gamage (Technical Officer, School of Minerals and Energy Resources Engineering, UNSW) for his assistance with the experimental setup and data collection.

REFERENCES

[1] S. Kumar Singh, B. Pratap Banerjee, and S. Raval, "A review of laser scanning for geological and geotechnical applications in underground mining," (in English), Int. J. Min. Sci. Technol., Review vol. 33, no. 2, pp. 133-154, 2023, doi: 10.1016/j.ijmst.2022.09.022.

[2] International Electrotechnical Commission (IEC), IEC System for Certification to Standards Relating to Equipment for Use in Explosive Atmospheres, Geneva, Switzerland: IEC, 2014.

[3] LEDinside;. "Hesai Unveils Breakthrough in In-Cabin LiDAR with IRR-CoatedWindshields." www.ledinside.com/news/2023/6/2023_06_05_01 (accessed May 11, 2025).

[4] U. o. C. B. Team 28, "Development of a Protective Enclosure for an Autonomous LiDAR System," University of Colorado Boulder, Department of Mechanical Engineering, 2022. [Online]. Available: www.colorado.edu/mechanical/team-28-protective-lidar-enclosure

[5] R. B. Biertümpfel, Ulf; Wolff, Frank, "Protective window in the optical path of a LIDAR system," in DGaO Proceedings, 2022: Deutsche Gesellschaft für angewandte Optik, p. B3.